

Interplay between group-delay-dispersion-induced polarization gating and ionization to generate isolated attosecond pulses from multicycle lasers

Carlo Altucci,^{1,*} Raffaele Velotta,¹ Valer Tosa,² Paolo Villorosi,³ Fabio Frassetto,³ Luca Poletto,³ Caterina Vozzi,⁴ Francesca Calegari,⁴ Matteo Negro,⁴ Sandro De Silvestri,⁴ and Salvatore Stagira⁴

¹CNISM–Dipartimento di Scienze Fisiche, Università di Napoli Federico II, via Cintia, 26—Ed. 6–80126, Napoli, Italy

²National Institute for R&D Isotopic and Molecular Technologies, Donath 69-103, 400293 Cluj-Napoca, Romania

³IFN-CNR and DEI-Università di Padova, via Gradenigo 6b, 35131 Padova, Italy

⁴IFN-CNR and Dipartimento di Fisica—Politecnico di Milano, Piazza Leonardo da Vinci 32, 20133 Milano, Italy

*Corresponding author: caltucci@unina.it

Received May 11, 2010; accepted June 28, 2010;

posted July 27, 2010 (Doc. ID 128301); published August 13, 2010

We implemented a new experimental scheme for the generation of single-shot extreme-UV continua that exploits a combination of transform-limited 15 fs, 800 nm pulses and chirped 35 fs, 800 nm pulses with orthogonal polarizations. Continua are interpreted as the formation of a single attosecond pulse and attributed to the interplay between polarization, ionization gating, and trajectory selection operated by suitable phase-matching conditions. © 2010 Optical Society of America

OCIS codes: 020.2649, 190.4160, 320.7110.

Different techniques have been demonstrated until now for generating single attosecond pulses (SAPs) that exploit high-order harmonic generation (HHG) by carrier-envelope phase (CEP) stabilized, few-cycle laser sources [1,2]. Recently, some efforts have been devoted to the extension of time-gating techniques to driving pulses in the multicycle regime [3,4]. In [3] the gate was formed just at the top of the overall field obtained by superposition of four field components with separately controlled phase and intensity and it led to the generation of a continuum extreme-ultraviolet (XUV) spectrum with 50 fs driving pulses. The scheme used in [4] exploits the combination of polarization and two-color gating and demonstrated generation of isolated attosecond pulses with 28 fs driving pulses. Another approach that has recently been proposed consists in HHG by a driving electric field with two orthogonally polarized components properly chirped and delayed [5]. In this case the gating is due to a combination of the driving electric field ellipticity, ionization, and trajectory selection operated by suitable phase matching. The tailoring of the driving pulse is such that it presents a time window of nearly linear polarization in the leading edge, corresponding to the maximum accessible laser intensity before ionization could deplete the gas target. This is a great advantage over the technique used in [3], as there is no need to wait for the top of the pulse, which imposes a severe limitation over the highest intensity that can be actually used for SAP generation. Width and time position of the gate window are controlled by the delay and the relative chirp of the two components and can be, in principle, positioned in any desired time location along the overall pulse. With respect to the previously mentioned techniques, the approach reported in [5] presents advantages such as easy implementation and robustness against laser-parameter fluctuations [6].

In this Letter we propose and experimentally demonstrate a significant improvement of our approach to SAP generation from multicycle driving lasers [5]. In fact, here the chirp of one of the two beams needed to realize sui-

table polarization gating was obtained by means of group delay dispersion (GDD), as in [7], rather than self-phase modulation (SPM), as suggested in [5]. This allowed us to relax the demand of a high SPM, which is not easy to achieve without significant temporal and spatial pulse distortion along the radial direction [6]. We also have carried out the experiment at higher intensity than that hypothesized in [5]; as a consequence, because the medium depletion takes place earlier, this leads to a narrower time window for harmonic generation.

Starting from a Ti:sapphire laser source (800 nm, 2 mJ), we achieved spectral broadening by filamentation in an Ar-filled gas cell and generated short pulses by chirped mirror compression. Typical duration and energy for these pulses are of the order of 15 fs and 1 mJ, respectively. We sent the pulses to a Michelson interferometer equipped with a computer-controlled delay line (minimum temporal resolution of 0.28 fs). In one arm of the interferometer we placed a broadband half-wave plate to rotate the polarization of the beam by 90° and a variable amount of glass for providing GDD and fine tuning of the gate window. This led the chirped pulse to a final duration of about 35 fs. Through a numerical simulation of the field propagation, we have estimated linear chirp and GDD coefficients as $\alpha \approx 2.7 \times 10^{-3} \text{ fs}^{-2}$ and $\beta \approx 140 \text{ fs}^2$, respectively. For a chirped Gaussian pulse, the relation between α and β is given by

$$\alpha = \frac{k^2\beta}{2(T_0^4 + k^2\beta^2)}, \quad (1)$$

where T_0 is the chirp-free pulse duration (FWHM) and $k = 4 \ln 2$. For $T_0 = 15 \text{ fs}$, Eq. (1) provides a maximum $\alpha \approx 3 \times 10^{-3} \text{ fs}^{-2}$, which is in fair agreement with our estimation for α , corroborating the evidence of optimal conditions in our experiment.

The two pulse components were recombined after the interferometer and sent to the generation chamber for

HHG. We focused the driving pulses on a synchronized gas jet with a spherical mirror having a 150 mm focal length. Characterization of harmonic emission was performed by means of a soft x-ray spectrometer and a microchannel plate coupled to a phosphor screen and a CCD camera. Because the laser source used in this experiment is not CEP stabilized, we acquired single-shot harmonic spectra in order to be able to observe the gating effects. The two pulse components separately generated harmonic emission in Kr with comparable spectral extension.

To illustrate the mechanism at work in our approach, we show in Fig. 1 the results of a simulation based on the strong field approximation [8] corresponding to our experimental parameters. The two components of the driving electric field are shown in Fig. 1(a). The GDD-induced phase term in the longer component was properly accounted for in the spectral domain. Figure 1(b) shows the total electric field ellipticity (solid curve) and the ionization fraction in krypton calculated with nonadiabatic Ammosov–Delone–Krainov (ADK) rates [9] (dashed curve). As can be seen, a gating window appears along the leading edge of the driving pulse, owing to the interplay between the modulation of the overall electric field polarization and the medium ionization depletion. In Fig. 1(c) the calculated single-dipole response (dashed curve) and the propagated harmonic field in the far field (solid curve) are depicted. The single-dipole response and the integration of the fundamental and harmonic propagation equations were performed in the time domain. Results reported in Fig. 1(c) clearly indicate the formation of a quasi-SAP, lasting ≈ 900 as after propagation in the far field, in correspondence of the timing of the gating scheme. A key role in the mechanism underlying SAP generation is played by both fundamental and harmonic field propagation through the target [10], which acts as a spatial filter contributing to temporally clean the final SAP. In fact, in the absence of propagation, the single-dipole response is made of three distinct pulses associated to the recombination originating from different electron trajectories [6].

Figure 2(a) shows a sequence of experimental harmonic spectra recorded as a function of the delay between the two driving pulses. The reported delay scan was obtained on a statistical basis, because the pulse CEP was not under control. In spite of CEP fluctuations, one can clearly see that a quasi-periodic modulation was induced in the harmonic yield for large delays; such modulation is due to the delay-dependent modulation in the polariza-

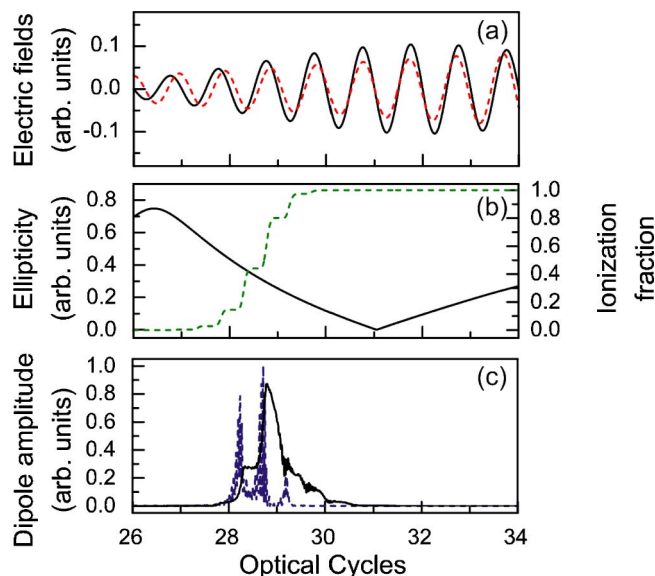


Fig. 1. (Color online) (a) Calculated perpendicularly polarized components of the electric field: 15 fs, 750 nm pulse (dashed curve) and chirped 33 fs, 750 nm pulse (solid curve). (b) Calculated ellipticity of the total driving field (solid curve, left vertical scale) and ionization fraction in krypton based on nonadiabatic ADK rates [10] (dashed curve, right vertical scale). (c) Calculated single dipole response (dashed curve) and propagated harmonic field in the far field (solid curve). The parameters of the simulations are a delay of 15 fs between the two pulses with the short pulse ahead; a CEP value of $\pi/8$ rad and $-\pi/8$ rad for the short and the long pulse, respectively; a peak intensity of about 8×10^{14} W cm $^{-2}$ for both pulses; and a GDD of ≈ 180 fs $^{-2}$ for the chirped pulse. As for the gas jet, the local pressure is 25 mbar, the length 0.6 mm—the jet being positioned 1 mm after focus in the diverging beams with a confocal parameter of 2.4 mm.

tion state of the overall driver, induced by the interplay between the tails of the two pulse components. One can also see that, for a delay of 15 fs (with the short pulse ahead in time) the generation of a continuous spectrum was obtained, whereas discrete and suppressed harmonics were observed just 0.5 fs later. This behavior is due to the fact that, in this range of delays, a tiny modification of the delay or of the CEP values of the pulses strongly affects the single electron dynamics, thereby switching close trajectories into open ones and vice versa. Around the delay of 15 fs, when the recollision is confined within the gate and the electric field triggers ionization depletion, one can observe the emission of a continuum spectrum in the 35–55 eV spectral region.

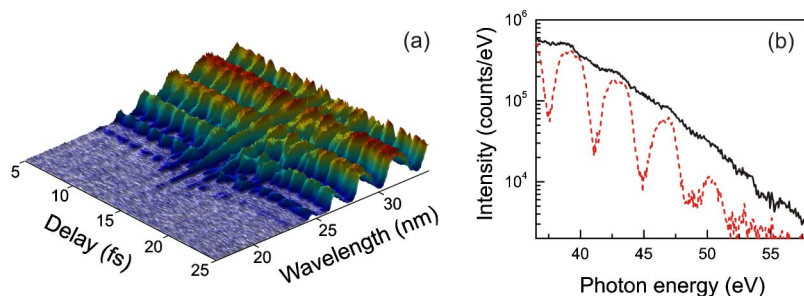


Fig. 2. (Color online) (a) Measured single-shot harmonic spectra in krypton for different delays between short and long pulse. (b) Single-shot harmonic spectra generated in krypton for delays of 15 fs (solid curve) and 15.5 fs (dashed curve), respectively, between the short and the long driving pulse (short pulse ahead) in conditions similar to those simulated in Fig. 1.

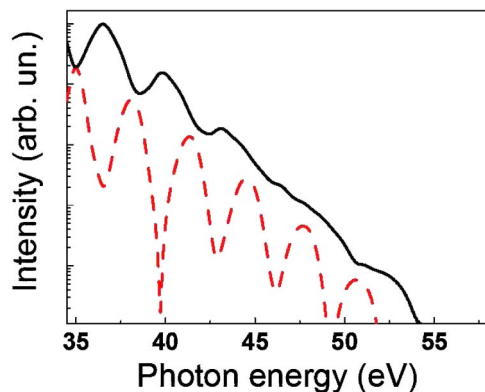


Fig. 3. (Color online) Simulated harmonic spectra in krypton for delays of 15 fs (solid curve) and 15.5 fs (dashed curve), respectively, between the short and the long driving pulse (short pulse ahead) in conditions similar to those used for Fig. 1 and corresponding to the measured spectra reported in Fig. 2(b).

Figure 2(b) shows in detail two XUV spectra acquired for a time delay of 15 fs (solid curve) and 15.5 fs (dashed curve) respectively, with the short pulse ahead in time. These spectra correspond to the maximum intensity of the electric field in the gate window, in a condition similar to that simulated in Fig. 1. A broad continuum is obtained in the former case, whereas discrete harmonics corresponding to several emission events are clearly visible for a delay of 15.5 fs. Similar effects, not shown, have been observed in argon. It is worth stressing that, as the pulse CEP changed from shot to shot, and the success of our scheme depends on the pulse CEP, we could not observe continua each time for a selected delay between the two pulses. Thus, for some configurations and specific delays, such as the one reported in Fig. 2(b), we acquired several consecutive shots observing continua in about 3%–5% of the cases, which reflects the statistical fluctuations of initial pulse CEP value. Our simulations indicate that CEP needs to be stabilized within ≈ 150 – 200 mrad to yield a robust SAP formation. The continuum bandwidth of the spectrum shown in Fig. 2(b) is wide and would support an SAP duration much shorter than the one of 900 as that we calculated. This pulse lengthening is due to a consistent chirp of the XUV pulse, which causes pulse lengthening, as predicted for analogous conditions [6].

Figure 3 shows the calculated spectra corresponding to the same conditions of the measurements reported in Fig. 2(b). In the simulations, the CEP values of the initial pulses, as well as all the other parameters, were chosen to be the same as for the simulations shown in Fig. 1. The agreement between measured and theoretical spectra (calculated in the experimental conditions) is very good, strongly corroborating our theoretical analysis. It turned out that our approach to generate SAPs from multicycle lasers not only depends on the CEPs of the initial pulses but also requires us to properly work a difference of about $\pi/4$ between the CEP values of the two pulses,

regardless of the sign of such a difference. This CEP difference is likely due to the phase cumulated, in correspondence of the carrier wavelength, by one of the two pulses that crossed the fused silica wedges to be properly chirped.

We mentioned that similar results were obtained also in argon, but continua were, in that case, less regular and spectrally extended and statistically more rare compared to what was observed in krypton. This is likely due to the fact that argon is harder to ionize compared to krypton; thus, the time confinement due to heavy ionization of the medium that acts as the rising arm of the time gate is, for argon, less efficient.

In conclusion, we have experimentally demonstrated that our method leads to XUV continuum generation, thanks to a novel physical interplay among polarization and ionization gating, strictly combined with 3D transient phase matching, starting from multicycle commercially available laser sources. The experimental scheme is easy to implement in a typical ultrafast laser facility and therefore represents a crucial step to enable the access to attoscience to a wide scientific community.

We acknowledge the financial support from the Italian Ministry of Research under project PRIN 2006027381 and the partial support from the European Commission Seventh Framework Programme (LASERLAB-EUROPE, grant agreement 228334).

References

1. E. Goulielmakis, M. Schultze, M. Hofstetter, V. S. Yakovlev, J. Gagnon, M. Uiberacker, A. L. Aquila, E. M. Gullikson, D. T. Attwood, R. Kienberger, F. Krausz, and U. Kleineberg, *Science* **320**, 1614 (2008).
2. G. Sansone, E. Benedetti, F. Calegari, C. Vozzi, L. Avaldi, R. Flammini, L. Poletto, P. Villoresi, C. Altucci, R. Velotta, S. Stagira, S. De Silvestri, and M. Nisoli, *Science* **314**, 443 (2006).
3. P. Tzallas, E. Skantzakis, C. Kalpouzos, E. P. Benis, G. D. Tsakiris, and D. Charalambidis, *Nat. Phys.* **3**, 846 (2007).
4. X. Feng, S. Gilbertson, H. Mashiko, H. Wang, S. D. Khan, M. Chini, Y. Wu, K. Zhao, and Z. Chang, *Phys. Rev. Lett.* **103**, 183901 (2009).
5. C. Altucci, R. Esposito, V. Tosa, and R. Velotta, *Opt. Lett.* **33**, 2943 (2008).
6. V. Tosa, K. Kovacs, C. Altucci, and R. Velotta, *Opt. Express* **17**, 17700 (2009).
7. F. Schapper, M. Holler, L. Gallmann, and U. Keller, presented at the Second International Conference on Attosecond Physics (Manhattan, Kansas, USA, 28 July–1 August 2009), paper S02.
8. M. Lewenstein, Ph. Balcou, M. Yu. Ivanov, A. L'Huilier, and P. B. Corkum, *Phys. Rev. A* **49**, 2117 (1994).
9. M. V. Ammosov, N. B. Delone, and V. P. Krainov, *Sov. Phys. JETP* **64**, 1191 (1986) [*Zh. Eksp. Teor. Fiz.* **91**, 2008 (1986), in Russian].
10. V. Tosa, K. T. Kim, and C. H. Nam, *Phys. Rev. A* **79**, 043828 (2009).